Supporting Information

Single Molecule Ionic Current Sensing in Segmented Flow Microfluidics

T. R. Gibb[†]*, A. P. Ivanov*[†]*, J. B. Edel*[†] *and T. Albrecht*[†].

[†]Department of Chemistry, Imperial College London, South Kensington Campus, London, SW7 2AZ.

Detailed Methods

Glass Nanopore Fabrication

Glass nanopores were pulled on a laser pipette puller (P200, Sutter Instruments, USA) using quartz capillaries with filament (ID: 0.5 mm, OD: 1 mm, Length 7.5 cm, Sutter Instruments). Pipette pulling occurs via a two step program using parameters: HEAT: 575, FIL: 3, VEL: 35, DEL: 145 and PULL: 75 followed by HEAT: 700, FIL: 0, VEL: 15, DEL: 128 and PULL: 200. The first step pulls a 1.2 mm taper into the capillary before the second forms the nanopore itself. In our experience these parameters are highly machine and room temperature specific hence the parameters cited can only be used as a guide for pipette fabrication.

Microfluidic Device Fabrication and Glass Nanopore Integration

Standard soft lithography methods were used to fabricate the microfluidic device. PDMS pre-cursor was poured over a SU-8 silicon master and cured on a hot plate. The cured PDMS chip and a 1 mm thick glass slide were plasma cleaned and bonded together with the glass slide sealing off the microfluidic device. Glass nanopores, pre-filled with KCl solution, were then manually inserted into the microfluidic device before a two part silicon rubber (00-30 Silicon Rubber Compound, Ecoflex) was used to seal the gap between the glass nanopores and the PDMS chip.

Microfluidic Measurements

In all experiments fluorinated oil (Fluorinert FC-40, 3M) with 2.5% by weight surfactant[1] was used as the carrier fluid. KCl (VWR) solutions were made with ultrapure water and filtered using a 0.2 micron lure lock syringe filter to remove any large particulate contamination. Fluids were

introduced into the microfluidic device using 1 ml plastic syringes (BD 1 ml, Plastipak) mounted on syringe pumps (PHD 2000, Harvard Apparatus, UK) using electrically shielded soft tubing (PTFE 59-8324, Harvard Apparatus, UK) with the tubing outlet connected to the PDMS microfluidic device inlet. Each device was flushed with the continuous oil phase for five minutes before experimentation to ensure the channel walls were fully coated in the oil phase and, in addition, upon changing the flow velocity the system was allowed to stabilize for two minutes before any measurements were taken to ensure accurate results. For experiments where changes in flow or KCl concentration were required data sets were collected in a random order to prevent any variation of device properties over time skewing the measured results.

Ionic current was measured with freshly chloridised Ag/AgCl electrodes wade from silver wire (0.125 mm diameter, Goodfellow, UK), one electrode inserted per glass nanopore. The microfluidic device was placed inside a Faraday cage with a dedicated low noise ground connection and all equipment connected to the device placed on a vibration isolation table. Biases were applied and currents measured with an Axopatch 200b low noise current amplifier (Axon Instruments, USA) in the voltage clamp mode. The collected data was low-pass filtered at 10 kHz using the built in 8 pole Bessel filter and the output signal sent to a Digidata 1440A data acquisition module (Axon Instruments, USA). The data was digitized at 50 kHz and recorded using pClamp 10.2 software before analysis was carried out using Clampfit 10.2 and Matlab 2013a.

Videos of the droplets in the microfluidic channel were obtained via a high speed camera (Phantom v5.1, Vision Research, USA) at 10,000 frames per second. Image analysis was carried out with a combination of Image-J and a custom, home written Matlab analysis routine.

DNA translocation studies were carried out with 10 kbp double stranded DNA (individual fragments from 1kbp DNA ladder obtained as a custom order form New England Biolabs Inc, USA). DNA samples were diluted to a 0.5 pM concentration in a buffer of 1 M KCl, 10 mM Tris and 1 mM EDTA electrolyte previously filtered using a 0.2 micron lure lock syringe filter. In all cases droplets were created with a control solution of DNA free buffer and a baseline taken before buffer containing DNA was used to create droplets and data recorded.

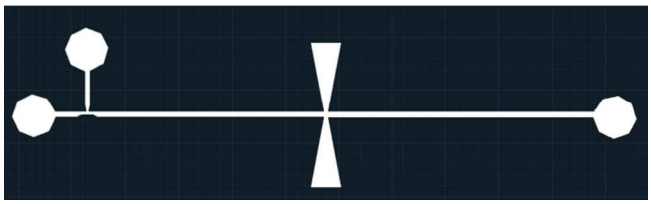

Figure S-1: Overview of the device geometry. Devices had a main channel width of 100 μm in all areas except for those involved in droplet generation where the channels narrowed to 50 μm. The two access shafts used to insert the glass nanopores into the microfluidic channel can be seen at the centre of the device.

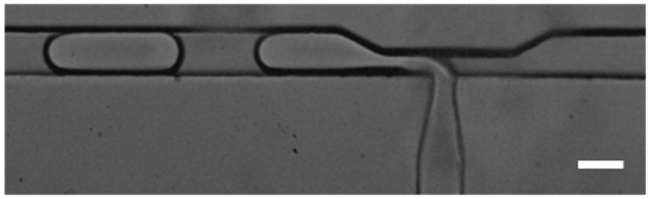

Figure S-2: Droplet generation at a flow velocity of 10 mm s^{-1}. Scale bar is 100 μm. Video also included online as a web enhanced object.

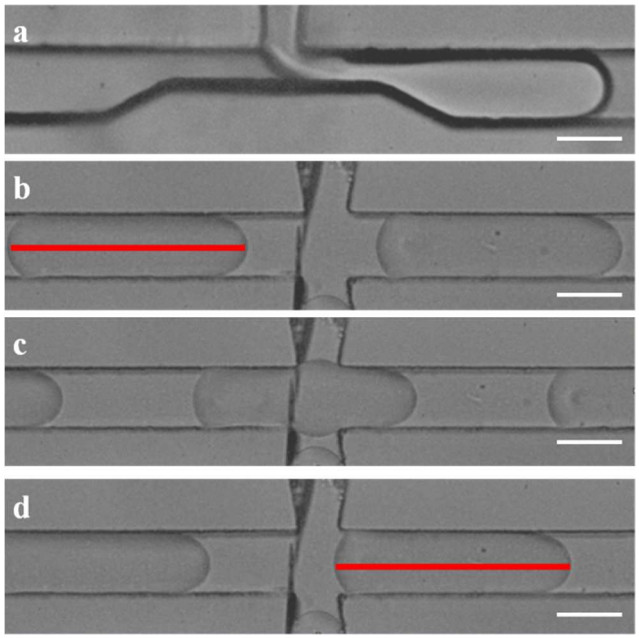

Figure S-3. Optical images of droplet production (a), transport (b and d) and detection (c). All images were taken at a flow rate of 10 mms^{-1} with an applied voltage of 500 mV Note that the red line in b and d is the same length, indicating the droplet suffers no permanent deformation after its passage through the detection area. Scale bars are all 100 μm.

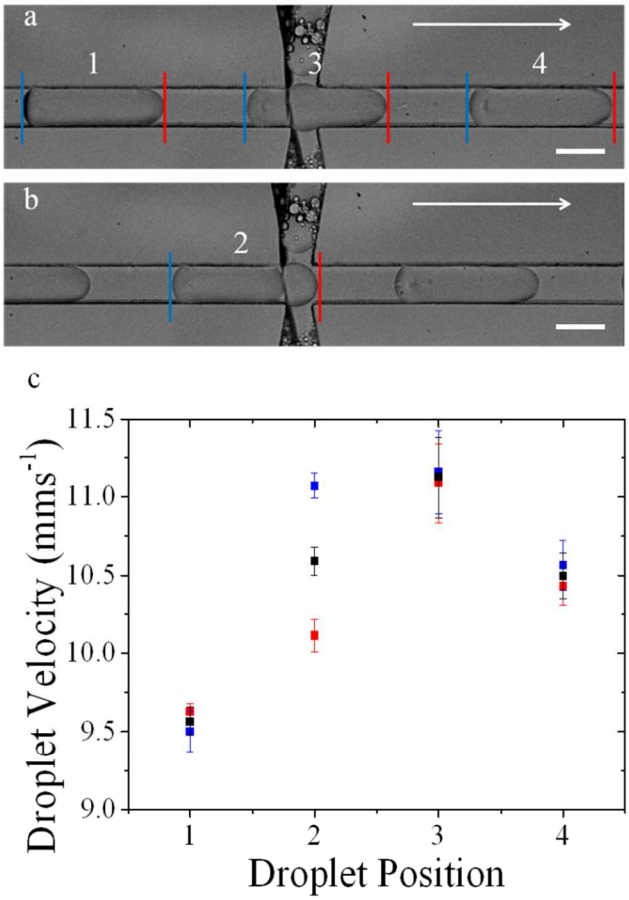

Figure S-4: (a and b) Measurement of droplet velocity in 4 locations in the device: 1, in the main channel before the glass nanopores, 2, in the area of the glass nanopores before droplet piercing, 3, in the area of the glass nanopores after droplet piercing and 4, in the main channel after the glass nanopores. In each location the velocity of both the leading and trailing droplet edges were measured at point denoted by red and blue lines respectively. Arrows indicate the direction of flow and the scale bar is 100 μm. (c) Average velocity at each of the four locations for the droplet's leading edge (red data points), trailing edge (blue data points) and the droplet as a whole (black data points) showing an increase in droplet velocity around the glass nanopores. Error bars are the standard deviation of the droplet velocity in all cases.

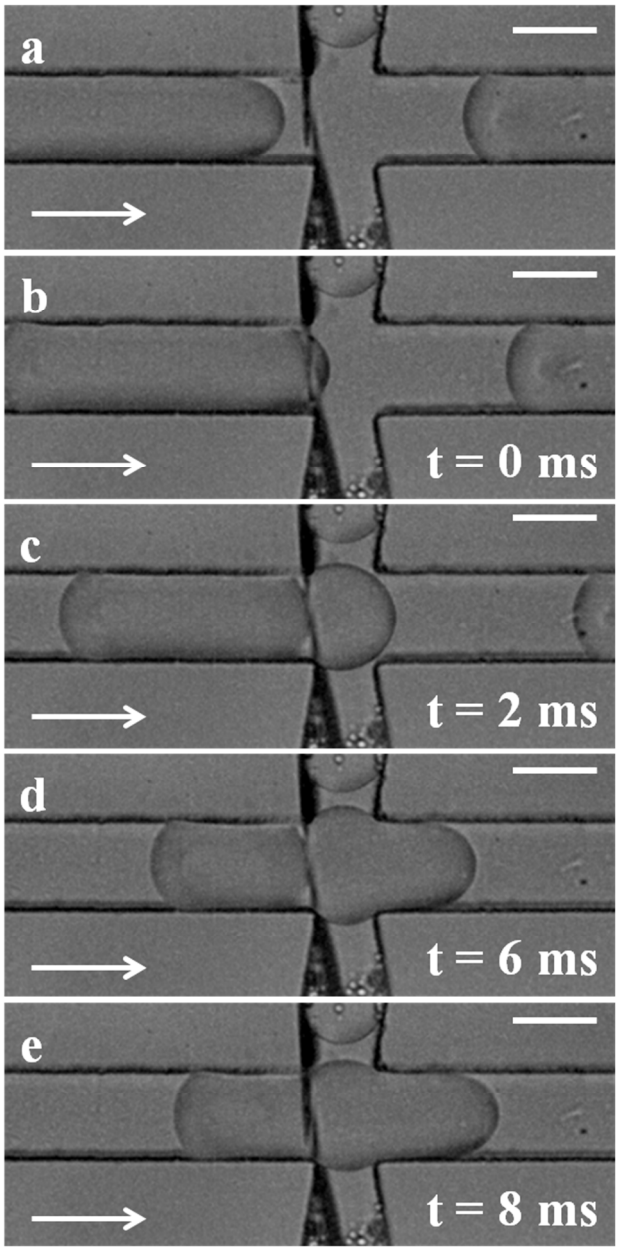

Figure S-5: Passage of a droplet at a flow velocity of 30 mm s^{-1} past the glass nanopores. Upon contact with the glass nanopores (b) the droplet's shape can be seen to be distorted just in front of the nanopores (c and d) before the droplet is pierced and the distortion disappears (e). The timescale for piercing here is 8 ms, the same timescale as the current spike seen at the beginning for droplets in some current time traces. All scale bars 100 µm. Video also included online as a web enhanced object.

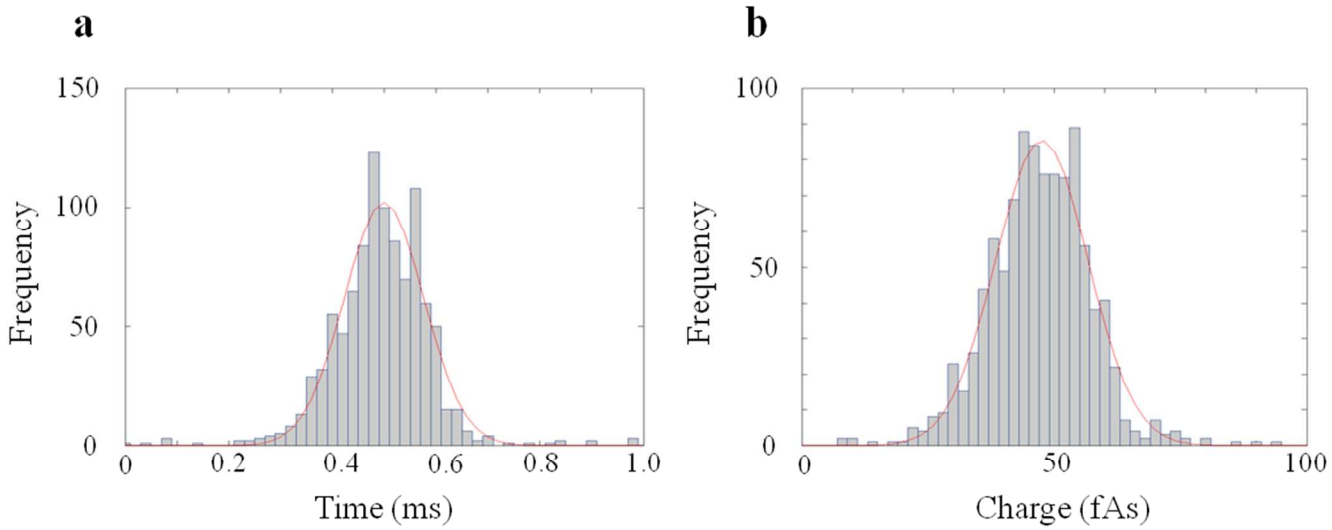

Figure S-6: Translocation data for a single nanopipette in an electrolyte of 1M KCl, 10mM Tris and 1 mM EDTA containing 0.5 pM 10 kb dsDNA, total volume 1 ml. In a one minute experiment, 1007 DNA translocation events were detected with a mean dwell time of 0.50 ± 0.10 ms and a mean integrated charge of 47.53 ± 4.77 fAs giving an analyte detection efficiency of ~0.0003% for the experiment.

The Potential for Nanopore Based Droplet Analysis

The recorded number of translocation events per droplet is affected by the flow velocity (hence the velocity of the droplets) and the translocation characteristics of the nanopore as well as the analyte. In the present case, the droplet residence time is on the order of 80 ms at a flow velocity of 5 mm s^{-1}; based on our data, the latter could be reduced to about 2.5 mm s^{-1} without compromising the droplet size distribution. This implies that the residence time could be increased to 160 ms. With regards to the translocation characteristics of pore and analyte, the situation is rather complex. For linear double-stranded DNA, the capture rate was found to be dependent on the length of the DNA (for DNA smaller than ~10 kbp); on the applied voltage (exponential dependence); the salt concentration gradient across the pore, and the DNA concentration (linear dependence).[2] For a given molecule, e.g. 10 kbp linear DNA as in the present case, all of the remaining three factors may be exploited to enhance the translocation frequency. The bias voltage arguably shows the strongest functional dependence, but at the same time cannot be increased significantly beyond the values used here (up to 600 mV). It should also be noted that in our setup the applied bias voltage drops at both nanopipettes, decreasing the local electric field at a single pipette to about 50%, compared to a single-pipette configuration. Moreover, large voltages result in short translocation times, which are more difficult to record and analyse. A voltage-induced enhancement of the translocation frequency beyond a factor of 2 or 3 thus seems unlikely. The effect of a salt gradient is similar in magnitude, if the DNA is translocated from a droplet with c(KCl) = 0.1 M into the

pipette with c(KCl) = 1.0 M.[2] Based on our present data, the concentration effect is expected to be largest. Using a radius of gyration of approximately 250 nm,[3] we estimate the molecular overlap concentration to be on the order of 0.1 nM, corresponding to about 276,000 molecules/droplet. In our experiments, we have used a DNA concentration of 0.5 pM (or 1300 molecules/droplet), which resulted in an average translocation frequency of 1.7 s^{-1} (averaged over all droplets, i.e. including those not showing any events). Overall a ~1600 fold increase in the translocation frequency could be expected, in principle allowing for nanopore-based analysis of single droplets.

(1) Draper, M.; Niu, X.; Cho, S.; James, D.; Edel, J. B. *Anal. Chem.* **2012**, *84*, 5801–5808.

(2) Wanunu, M.; Morrison, W.; Rabin, Y.; Grosberg, A. Y.; Meller, A. *Nat. Nanotechnol.* **2010**, *5*, 160–5.

(3) Robertson, R. M.; Laib, S.; Smith, D. E. *Proc. Natl. Acad. Sci. U. S. A.* **2006**, *103*, 7310–4.